

# Failure Mechanism of Lead-Free Solder Joints in Flip Chip Packages

FAN ZHANG,<sup>1</sup> MING LI,<sup>1</sup> BAVANI BALAKRISNAN,<sup>1</sup>  
and WILLIAM T. CHEN<sup>2</sup>

1.—Institute of Materials Research and Engineering (IMRE), Singapore 117602. 2.—ASE (US) Inc., Santa Clara, CA 95054.

The failure mechanisms of SnAgCu solder on Al/Ni(V)/Cu thin-film, under-bump metallurgy (UBM) were investigated after multiple reflows and high-temperature storage using a ball shear test, fracture-surface analysis, and cross-sectional microstructure examination. The results were also compared with those of eutectic SnPb solder. The Al/Ni(V)/Cu thin-film UBM was found to be robust enough to resist multiple reflows and thermal aging at conditions used for normal production purposes in both SnAgCu and eutectic SnPb systems. It was found that, in the SnAgCu system, the failure mode changed with the number of reflows, relating to the consumption of the thin-film UBM because of the severe interfacial reaction between the solder and the UBM layer. After high-temperature storage, the solder joints failed inside the solder ball in a ductile manner in both SnAgCu and SnPb systems. Very fine Ag<sub>3</sub>Sn particles were formed during multiple reflows in the SnAgCu system. They were found to be able to strengthen the bulk solder. The dispersion-strengthening effect of Ag<sub>3</sub>Sn was lost after a short period of thermal aging, caused by the rapid coarsening of these fine particles.

**Key words:** Flip chip, under-bump metallurgy (UBM), SnAgCu solder, interfacial reaction, (Cu,Ni)<sub>6</sub>Sn<sub>5</sub> ternary compound

## INTRODUCTION

Flip chip technology has been addressed as an important technology in the packaging industry in the semiconductor roadmap.<sup>1</sup> Flip chip solder-bump interconnection provides electrical and mechanical connections between the Si die and package and is regarded to be more suitable for high input/output numbers and small size components.<sup>2,3</sup> Thus, the drive for miniaturization of components and devices has shifted the attention to the flip chip technology. The key component in the flip chip interconnection system is the thin-film, under-bump metallurgy (UBM). The thin-film UBM consists of multilayers, which are chosen based on three criteria: a good wetting layer to the solder, an efficient barrier layer to the diffusion of solder, and a reliable adhesion layer to chip metallization.<sup>2-4</sup> The thin-film UBM should be robust enough to resist several runs of reflows (wetting reaction) for assembly and long peri-

ods of thermal aging (solid-state diffusion) for service. The integrity of thin-film UBM is, therefore, crucial to the reliability of flip chip packages.

The Pb-bearing solders have been widely used in the electronic packaging industry for a long time. However, because of the detrimental effects of Pb to the environment, exigent measures have been taken to reduce and, in the near future, totally phase out the usage of Pb in production. While the industry is moving towards Pb-free production, there are more challenges encountered in elucidating an appropriate UBM system for flip chip interconnections. The Pb-free solder candidates, such as SnAg, SnCu, or SnAgCu, usually contain a higher percentage of Sn and possess higher melting points compared to that of the commonly used eutectic SnPb solders. This brings up two crucial issues during production: higher reflow temperatures and severe interfacial reactions between the solder and the UBM.<sup>5,6</sup> The conventional Cr/CrCu/Cu-based UBM is found to no longer be compatible because of the fast spalling of intermetallics from the interface. The Ni-scheme

(Received February 11, 2002; accepted May 16, 2002)

UBM, thus, emerged mainly because of the slow reaction rate between Sn and Ni.<sup>7-9</sup> Among them, Al/Ni(V)/Cu UBM has attracted more and more interest recently.<sup>10,11</sup> In this UBM system, Cu acts as a solderable layer to the solder and Ni as a diffusion barrier. It needs to be mentioned that V is cosputtered with Ni during the process to mitigate the magnetic interference of Ni and to speed up the fabrication process.<sup>10</sup> Moreover, it was found that Ni (V) UBM could form a very low energy interface with  $\text{Cu}_6\text{Sn}_5$  intermetallic compounds (IMCs) and prevent the spalling of IMCs from the solder/UBM interface.<sup>10</sup> Although the Ni (V) UBM has been proven to be reliable to eutectic SnPb solders, its behavior in Pb-free systems has not yet been well established. It will be interesting to study the interaction of thin-film Ni (V) UBM with Pb-free solders where higher processing temperatures are involved.

In this paper, interfacial reactions during multiple reflows and thermal aging between Sn3.5Ag1.0Cu Pb-free solder and Al/Ni(V)/Cu UBM were studied. High-resolution field-emission gun (FEG) scanning electron microscopy (SEM) was used to monitor the evolution of the thin-film Ni (V) UBM. Ball shear tests were conducted to evaluate the solder joint's reliability. Possible failure mechanisms for the Pb-free solder joint were discussed.

## EXPERIMENTAL PROCEDURE

Two types of solders, Sn3.5Ag1.0Cu and eutectic SnPb (as a control), were bonded to thin-film Al/Ni (V)/Cu UBM on an Si die, as illustrated in Fig. 1. The total thickness of the thin-film UBM is about 1  $\mu\text{m}$ . The diameter of the formed solder ball is about 120  $\mu\text{m}$ , while its bump height is around 100  $\mu\text{m}$ . Some of the as-bonded dies were subjected to thermal aging at 150°C for up to 1,000 h, while the rest of them were used for multiple reflows. Although normal packages rarely experience more than 5 runs of reflow during the production process, we extended the number up to as many as 30 in the Pb-free system to study the interfacial reaction between the Pb-free solder and the thin-film Ni (V) UBM at extreme cases. The reflow treatments were performed in a BTU SS70 five-zone reflow oven in  $\text{N}_2$  atmos-

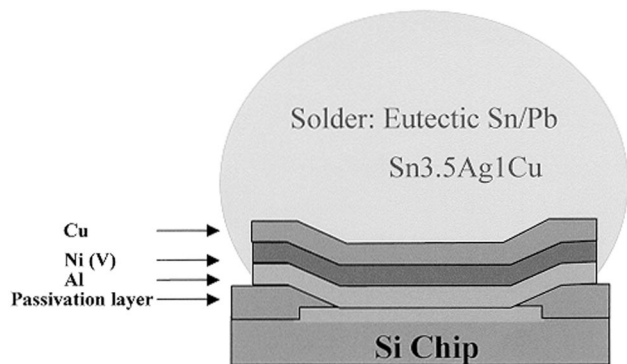


Fig. 1. The schematic diagram of the test die showing layout of Al/Ni (V)/Cu thin film UBM.

phere. The  $\text{O}_2$  level was kept below 50 ppm. The peak temperatures were 260°C and 220°C for SnAgCu and eutectic SnPb solders, respectively, and reflow time (time above melting point of the solder in each reflow) was about 60–65 sec.

The heat-treated samples (multiple reflows and thermal aging) were then subjected to ball shear tests using a Dage 4000 series tester (U.K.), with a shear speed of 200  $\mu\text{m}/\text{sec}$  and shear height of 10  $\mu\text{m}$ . An average of shear forces of 44 solder bumps was taken for each condition. Fracture surfaces were analyzed under SEM.

For cross-sectional observations, heat-treated samples were cold-mounted into epoxy resin and cured at room temperature. The mounted samples were ground and polished using diamond paste down to 1  $\mu\text{m}$ . A high-resolution Jeol JSM-6700F FEG SEM (Japan), equipped with an Oxford Instrument (U.K.) energy dispersive x-ray analyzer (EDAX), was used to monitor the thin-film UBM evolution and phase compositions. Time for signal collection in each elemental line scan was about 10 min.

## EXPERIMENTAL RESULTS

### Microstructural Evolution

#### *Microstructure Evolution during Multiple Reflows*

*SnAgCu System:* The microstructures of samples after different numbers of reflow are shown in Fig. 2a-d. It was found that the  $\text{Cu}_6\text{Sn}_5$  IMC formed on top of the Ni (V) UBM after the first reflow (Fig. 2a). The majority of IMCs was scalloplike in shape and adhered well to solder/UBM interfaces. The IMCs were also found floating above those that adhered to the solder/UBM interfaces and precipitated inside the bulk solder. The Ni (V) UBM thin film was nearly intact after initial reflow. No trace of Ni could be detected in the  $\text{Cu}_6\text{Sn}_5$  IMC.

With the increase of reflow number to more than five, as shown in Fig. 2b and c, “white patches” were found to appear discontinuously inside the Ni (V) UBM layer. It could be expected that the appearance of white patches implied a start of the consumption of the UBM thin film. The EDAX results show that the majority of the elements in these regions were Sn and V, although a small amount of Ni could still be detected, which confirmed the loss of Ni from the UBM layer, as clearly shown in Fig. 2e and f. It was found that the percentage of white patches in UBM increased with reflow numbers. Only a small amount of white patches could be observed, and the adhesion between solder and UBM was good within five reflows, which meant that Ni (V) was a good diffusion barrier for normal assembly process. To understand the mechanisms of Ni (V) UBM consumption during the reflows, some samples were subjected to 30 reflow cycles. It was interesting to find that even with the gradual increase of white

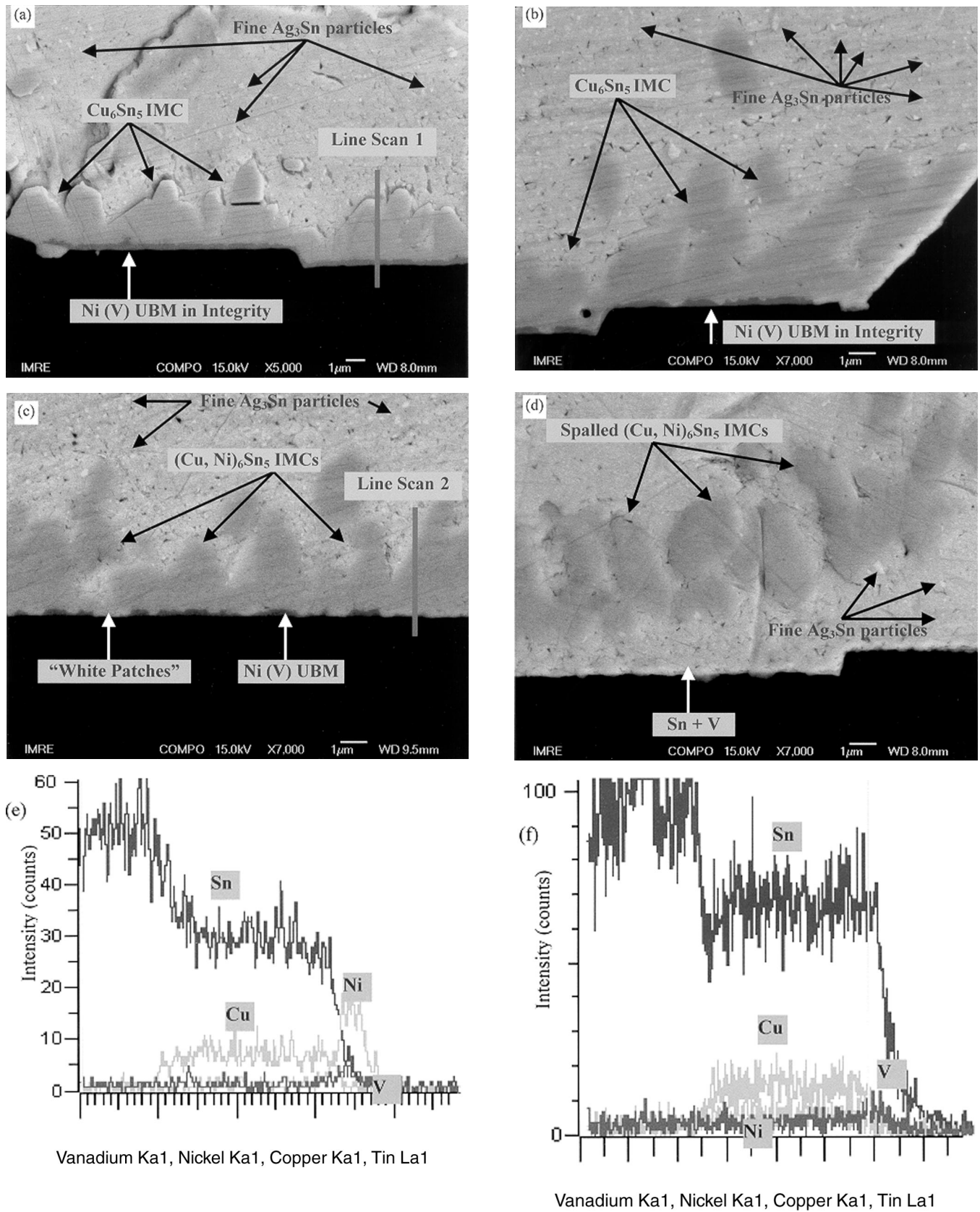


Fig. 2. The SEM micrographs of SnAgCu samples reflowed at 260°C after (a) 1 cycle, (b) 5 cycles, (c) 10 cycles, and (d) 30 cycles; EDAX line-scan results at (e) line 1 in Fig. 2a and (f) line 2 in Fig. 2c.

patches in the Ni (V) thin film with the number of reflows,  $\text{Cu}_6\text{Sn}_5$  IMCs still adhered well to the UBM layer. In the mean time, more and more Ni, which was originally located at the UBM, could be detected inside the  $\text{Cu}_6\text{Sn}_5$  IMCs. The EDAX results showed that about 8 at.% of Ni could be detected after 20 reflows in the  $\text{Cu}_6\text{Sn}_5$  IMC. The  $\text{Cu}_6\text{Sn}_5$  IMC has been converted to a ternary  $(\text{Cu}, \text{Ni})_6\text{Sn}_5$  phase, which is in agreement with results published by other researchers.<sup>12,13</sup>

The whole IMC layer, formerly adhered to the solder/UBM interface, finally spalled away and drifted into the bulk solder after 30 reflows (Fig. 2d). A layer of solder (Sn and  $\text{Ag}_3\text{Sn}$ ) could be observed between the IMCs and the Al layer in the UBM. The layered structure of Ni (V) could no longer be seen. It was also found that the IMC spalled as an agglomerated particle, where nearly all IMCs still stuck together after spalling. Compared to the spalling phenomenon in the  $\text{Cu}_6\text{Sn}_5$ -Cr/CrCu/Cu system,<sup>7</sup> dewetting might no longer be the main reason for the bulk IMC spalling in the current IMC Ni (V) UBM system. It is worth noting that not all the IMCs at the interface spalled after 30 reflows, IMCs adhering to Ni (V) UBM could still be observed in some areas.

In the bulk solder, very fine  $\text{Ag}_3\text{Sn}$  particles were found precipitated throughout the Sn matrix (Fig. 2). The particle size of the majority of  $\text{Ag}_3\text{Sn}$  was in the range of 150–300 nm, although bigger particles of about 500 nm and smaller particles of about 50 nm could also be seen. Our observations were consistent with that stated by Jang et al.,<sup>14</sup> in which they claimed to find  $\text{Ag}_3\text{Sn}$  in submicron size. Although the volume of the solder bump in the current study was very small and its solidification rate could be faster as compared to that in normal ball-grid array, it was still surprising to obtain such submicron particles after multiple reflows in flip chip solders. According to Jang et al.,<sup>14</sup> the larger degree of undercooling ( $\Delta T$ ) during reflow solidification of solder balls in flip chip packages might be the reason for obtaining fine  $\text{Ag}_3\text{Sn}$  particles. Large platelike  $\text{Ag}_3\text{Sn}$  phases could occasionally be observed in some solder bumps. Besides  $\text{Ag}_3\text{Sn}$ , some  $\text{Cu}_6\text{Sn}_5$ -based phases could be found precipitated in the bulk solder in large columnar or circular shapes.

**Eutectic SnPb System:** Contrary to the situation in the Pb-free system, the Ni (V) system was found to be very stable in the eutectic SnPb system, as demonstrated in Fig. 3a and b. After as many as 20 reflows at 220°C, the Ni (V) thin film showed no sign of being consumed. It was clearly seen as a good-layered structure. The  $\text{Cu}_6\text{Sn}_5$  IMC was in a scallop shape and covered the Ni (V) thin-film UBM very well. A negligible amount of Ni could be detected in the  $\text{Cu}_6\text{Sn}_5$ , which confirmed the integrity of the Ni (V) thin-film UBM. The results confirmed that the Ni (V) UBM was much more stable in the SnPb system during reflows than in the SnAgCu

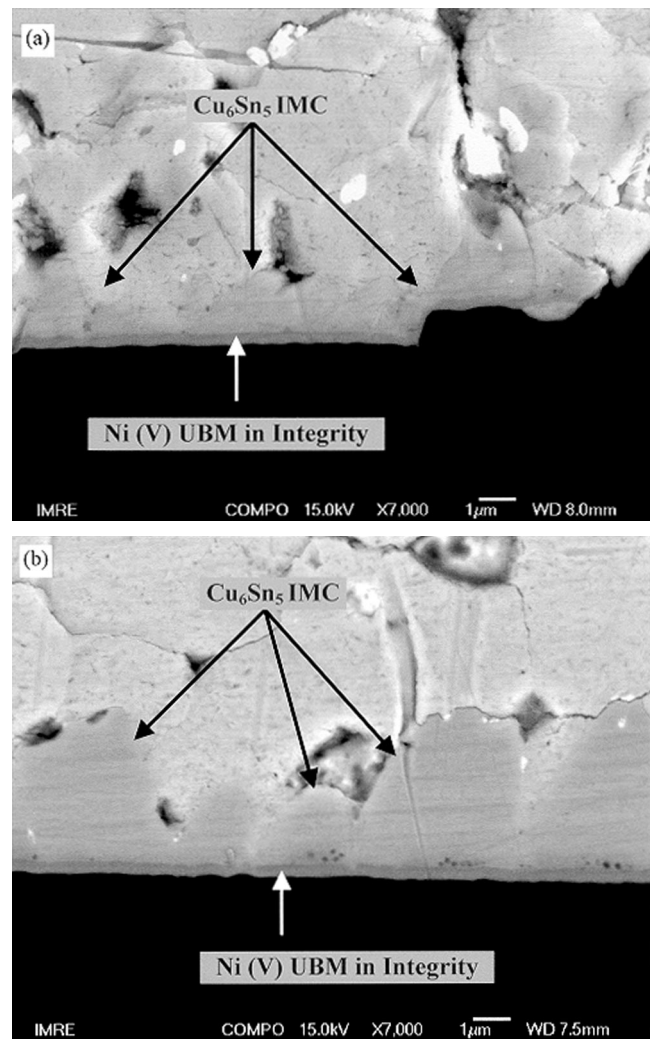


Fig. 3. The SEM micrographs of eutectic SnPb samples after (a) 1 reflow cycle and (b) 20 reflow cycles at 220°C.

system. This could mainly be ascribed to the less severe interfacial reaction between eutectic SnPb solder and Al/Ni (V)/Cu UBM because of the lower Sn content in the solder and the lower peak-reflow temperature.

Although the SnPb solder used in this study was of eutectic composition, the microstructure in the bulk solder was not a fully eutectic Sn-Pb lamella structure, and a certain amount of primary Pb (Sn) phase was found finely distributed throughout the bulk solder. This might be due to the relatively faster cooling rate of the smaller solder bump in the flip chip packages during the cooling stage of reflow.

#### *Microstructure Evolution after Different Periods of Thermal Aging at 150°C*

With an increase of the aging duration, Ni (V) was found to have a negligible reaction with the  $\text{Cu}_6\text{Sn}_5$  IMC at the interface, both in SnAgCu and the eutectic SnPb system, as shown in Figs. 4 and 5. It indicated that Ni, in the Ni (V) thin-film UBM, diffused very slowly to the  $\text{Cu}_6\text{Sn}_5$  layer in the solid-solid reaction. The Ni (V) UBM was, therefore, expected to

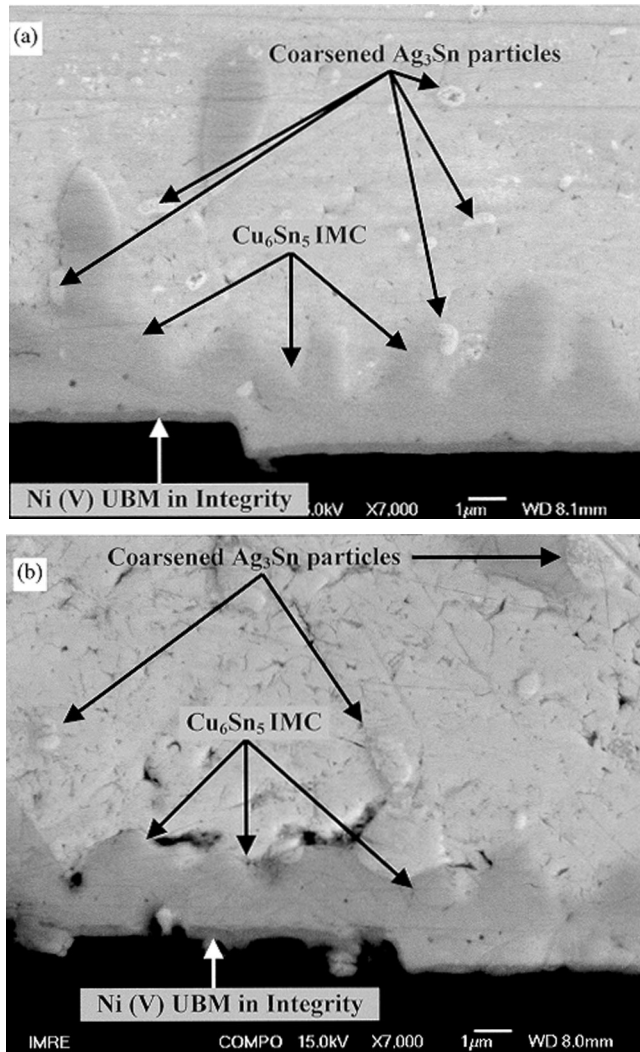


Fig. 4. The SEM micrographs of SnAgCu samples after aging at 150°C for (a) 4 h and (b) 500 h.

serve as a good diffusion-barrier layer under a high-temperature storage condition in the eutectic SnPb and the Pb-free solder systems. The prominent effect of aging in both systems could be seen from the morphology of  $\text{Cu}_6\text{Sn}_5$ . The morphology has changed from a scallop to a layered structure after 1,000 h of aging.

In the SnAgCu system, the ultrafine  $\text{Ag}_3\text{Sn}$  particles formed from multiple reflows rapidly during thermal aging. It could be observed from Fig. 4a that the particle size of  $\text{Ag}_3\text{Sn}$  increased to about 1  $\mu\text{m}$  with 4 h of aging at 150°C. The fast growth of  $\text{Ag}_3\text{Sn}$  particles was understandable. Because the fine  $\text{Ag}_3\text{Sn}$  particles possessed a large area of interface, they were in a high-energy nonequilibrium state. Thus, the driving force for the growth of the  $\text{Ag}_3\text{Sn}$  particle (coalescence) to decrease the interfacial energy and, therefore, the total energy of the system could be large during thermal aging. For the eutectic SnPb system, the primary Pb (Sn) phase was also coarsened to form a large “cluster” after thermal aging.

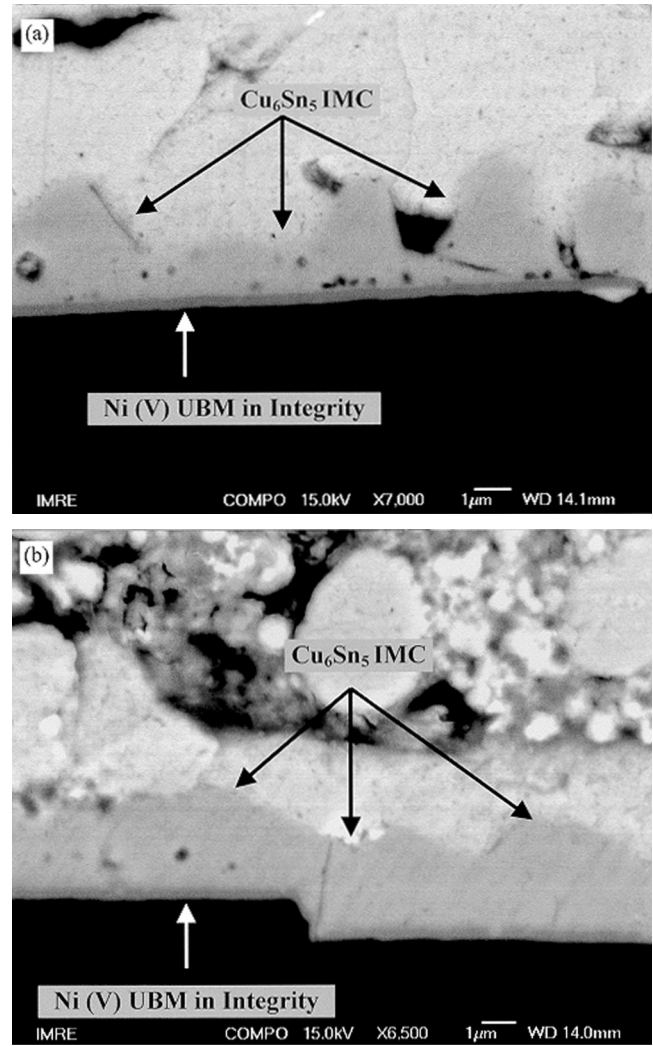


Fig. 5. The SEM micrographs of eutectic SnPb samples after aging at 150°C for (a) 24 h and (b) 500 h.

## Ball Shear Strengths of Solder Joints and Fracture Behavior

### Multiple Reflows

The ball shear strengths of samples after multiple reflows are shown in Fig. 6a. It could be seen that the shear strengths changed slightly with the number of reflows in the SnAgCu and the eutectic SnPb systems. However, the shear mode changed from ductile (failure inside the bulk solder) to partial brittle (failure at the solder/IMC or IMC/UBM interfaces) in the SnAgCu system with an increase of number of reflows to 30, as shown in Fig. 7. It can be seen that the solder failed at the IMC/UBM interface at the outer ring of the UBM, but the crack still passed through the bulk solder in the center area of the joint. Surprisingly, the completely brittle failure was not observed even after the spalling of the IMCs from the solder/UBM interface. The partial ductile failure in the center could be due to the design of the UBM structure of the test dies in the current study. There existed a step in the outer part of the UBM, as

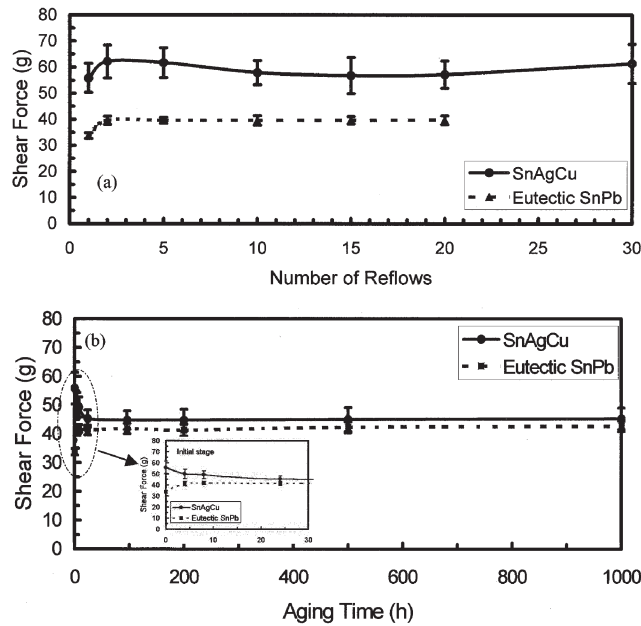


Fig. 6. The ball shear-test results of samples (a) after multiple reflows and (b) after thermal aging at 150°C.

shown in Fig. 1. During the shear tests, the crack might prefer to cross at the same level as the previous crack path (at the level of the UBM outer ring). This implied that the ball shear test might not be sensitive enough to detect changes of thin-film UBM in the present study.

For the eutectic SnPb system, the failure mode remained ductile after as many as 20 reflows, as shown in Fig. 8. This was consistent with UBM evolution observations. The shear strengths of the SnPb solder were found to be much lower than those of the SnAgCu solder. This could be due to the strengthening effect from a very fine, particulate  $\text{Ag}_3\text{Sn}$  phase in bulk SnAgCu solders.

#### Thermal Aging at 150°C

The ball shear strengths of samples after different periods of thermal aging are given in Fig. 6b. Different trends were found in the SnAgCu and SnPb systems. For the Pb-free system, the strength decreased immediately after thermal aging and stabilized after 24 h of aging. However, in the eutectic SnPb system, the strength increased at the initial stage of aging but stabilized afterwards. The decrease of strength in the SnAgCu system might be due to the coarsening of fine  $\text{Ag}_3\text{Sn}$  particles during aging (Fig. 4a) and, hence, the loss of its strengthening effect. Because the driving force for particle coarsening in the current study is large, as mentioned earlier, this process could proceed rapidly. However, it was surprising to see the increase of shear strength at the initial stage of aging in the SnPb system. This might be related to the morphological change of the Pb phase in the bulk solder. More studies are needed to clarify this phenomenon.

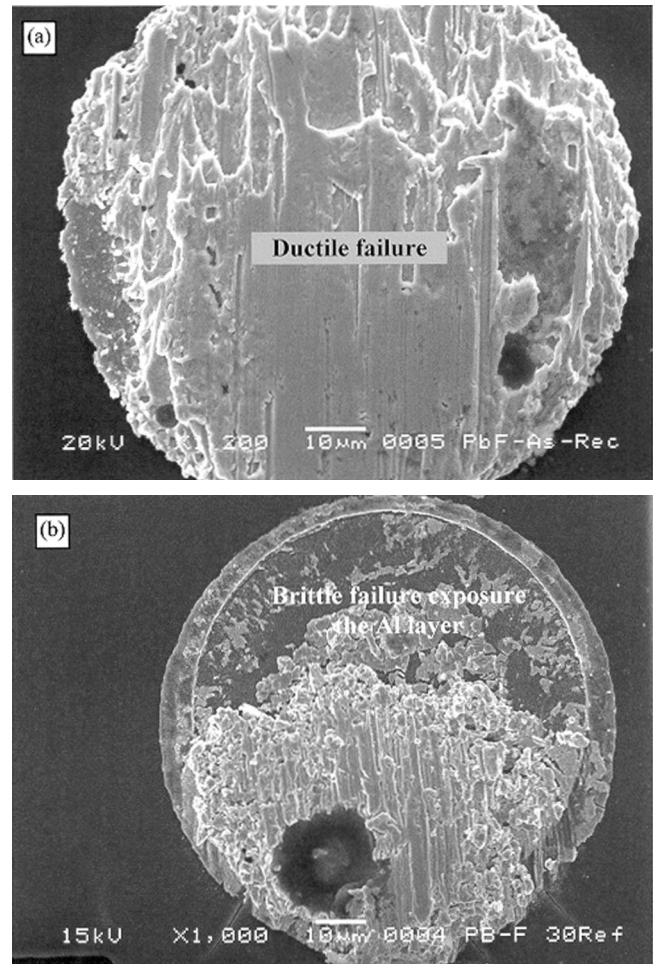


Fig. 7. The fracture surfaces of SnAgCu solder joints after (a) 1 reflow and (b) 30 reflows at 260°C.

All fractured surfaces of thermally aged samples indicated ductile-failure mode for both the Pb-free and SnPb system samples, as shown in Fig. 9.

## DISCUSSION

### Mechanisms of Ni (V) UBM Consumption during Multiple Reflows

To clarify the thin-film UBM consumption mechanism, the interaction between the IMC and the molten solder (solid-liquid reaction) during reflow process should be understood first. This is regarded as a complicated process and involves at least the following phenomena occurring simultaneously: (a) diffusion through the IMC bulk and scallop boundary, (b) IMC grain coarsening, (c) IMC grain-boundary grooving, and (d) dynamic local equilibrium of dissolution of the IMC into the molten solder and the formation of a solid IMC.<sup>15–17</sup> A possible mechanism<sup>18</sup> for Ni (V) UBM consumption is illustrated in Fig. 10. As shown in Fig. 10a,  $\text{Cu}_6\text{Sn}_5$  adhered well to the Ni (V) UBM after initial reflow. During the subsequent reflows, molten solder would interact with  $\text{Cu}_6\text{Sn}_5$  IMC and Ni, as illustrated in Fig. 10b. To consume the Ni (V) UBM, which is beneath

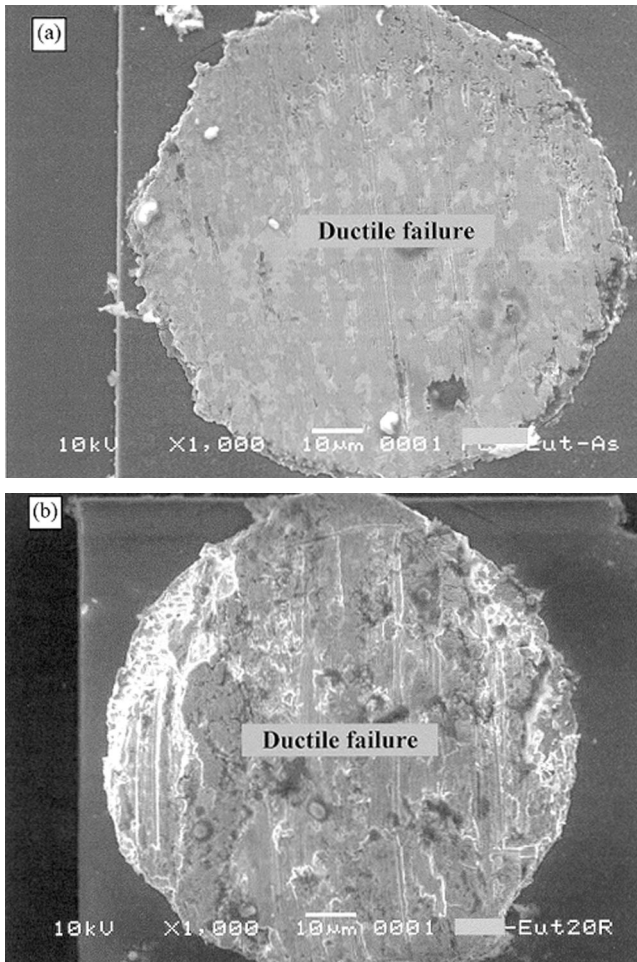


Fig. 8. The fracture surfaces of eutectic SnPb solder joints after (a) 1 reflow and (b) 20 reflows at 220°C.

$\text{Cu}_6\text{Sn}_5$  IMC, “liquid channels” between IMC scallops for molten solder to directly contact with Ni (V) must be created during reflow, as the diffusion through the bulk IMC is usually slow. This could be achieved through the grain-boundary grooving process. The rate of liquid-channel formation is estimated to be dependent on the thickness and morphology of the IMC, the rate of IMC boundary grooving, and the dissolution rate of the IMC into molten solder. After a liquid channel is opened for molten solder to flow through, Ni (V) could start to interact with the solder (Sn) and dissolve into the solder until the solubility limit is reached. The molten solder then can be regarded as an Sn (Cu, Ni) solution. During the cooling stage of the reflow process, the Sn (Cu, Ni) solution could precipitate as a (Cu, Ni) $_6\text{Sn}_5$  ternary phase instead of a binary  $\text{Cu}_6\text{Sn}_5$  phase. At the place where Ni (V) reacted with the molten Sn, the liquid channel would be closed up after the solidification. Therefore, the Sn was trapped inside the UBM area. White patches (caused by the higher atomic number of Sn than Ni) could, therefore, be seen in back-scattered electron mode under SEM micrographs, as shown in Figs. 2 and 10. With the increase of reflow cycles, the Sn

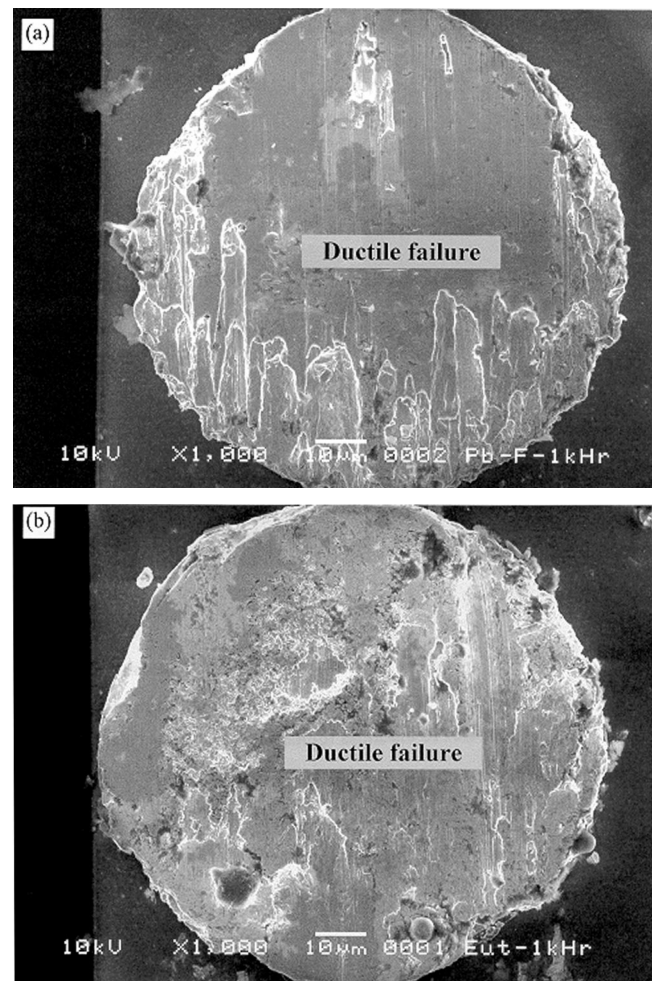


Fig. 9. The fracture surfaces of samples (a) SnAgCu and (b) eutectic SnPb solder joints after 1,000 h of aging at 150°C.

gradually replaced the Ni in the Ni (V) UBM and finally caused the spalling of the IMC, as indicated in Figs. 2 and 10.

#### Effects of Reflow Peak Temperature and Cu Solubility on Ni (V) UBM Consumption

As it was stated previously, IMC spalling could occur in the SnAgCu system after 30 reflows, while no such phenomenon could be found in the eutectic SnPb system. As shown early, the reflow temperature for the Pb-free solder (260°C) is 40°C higher than that of the eutectic SnPb solder. According to the phase-diagram calculation,<sup>18</sup> the solubility of Cu in the SnAgCu solder at 260°C is much higher than that in the eutectic SnPb solder at 220°C. The difference in Cu solubility is believed to affect the rate and amount of the  $\text{Cu}_6\text{Sn}_5$  IMC dissolved into the molten solder during reflow. It was expected that the lower Cu solubility at a reflow temperature of 220°C for the eutectic SnPb system might not be enough to create liquid channels for molten Sn directly contacting the Ni (V) layer. Therefore, no Ni (V) consumption at UBM could be found in this system. If the reflow peak temperature was increased to 260°C, white patches could also be observed even in

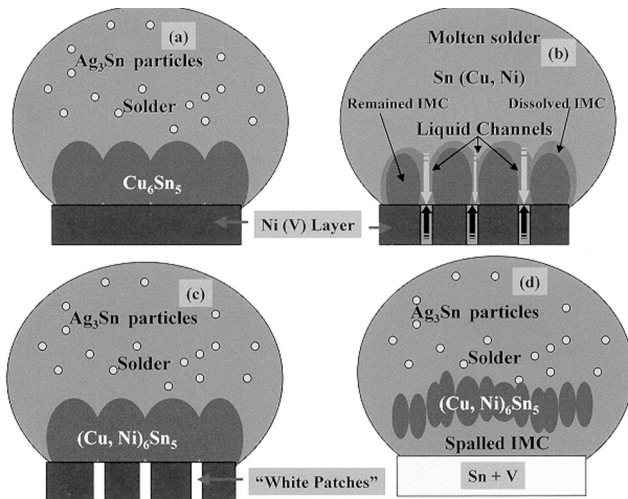


Fig. 10. The Ni (V) UBM consumption mechanism during multiple reflows: (a) after initial reflow, (b) during subsequent reflow, (c) after solidification of subsequent reflow, and (d) IMC spalling after enough numbers of reflows.

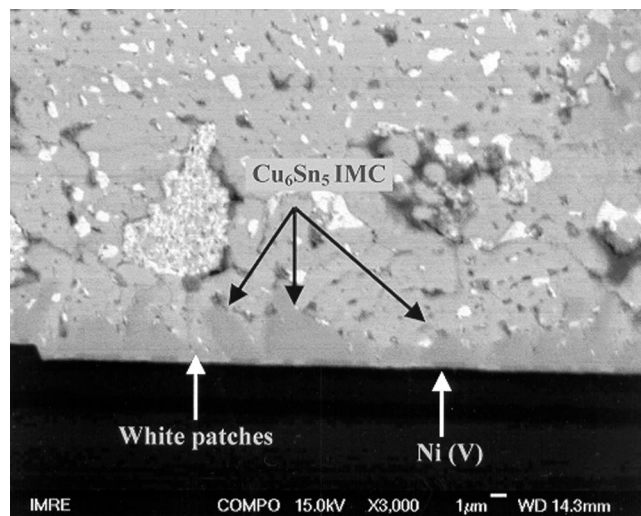


Fig. 11. The SEM micrograph showing the white patches in Ni (V) UBM in eutectic SnPb sample after 10 reflows at 260°C.

the eutectic SnPb system, as shown in Fig. 11. This implied that the peak reflow temperature in the assembly was of great importance to the integrity of the thin-film Ni (V) UBM. Therefore, process windows should be tightly controlled.

### CONCLUSIONS

- The Al/Ni (V)/Cu was found to be robust enough to resist multiple reflows in normal assembly processes (<5 reflows) in the SnAgCu and the eutectic SnPb systems
- The Al/Ni (V)/Cu was a good diffusion barrier to resist thermal aging at 150°C for up to 1,000 h in the SnAgCu and the eutectic SnPb systems
- Very fine Ag<sub>3</sub>Sn particles, in the range of tens to several hundreds of nanometers, were found precipitated throughout the Sn matrix in the SnAgCu system after multiple reflows. These

fine precipitates seemed to provide a dispersion-strengthening effect to the bulk solder. However, this effect was diminished after a short period of thermal aging because of the rapid coarsening of the Ag<sub>3</sub>Sn particles.

- Thin-film Ni (V) UBM was consumed gradually during the multiple reflows in the SnAgCu system, while it remained nearly intact in the eutectic SnPb system. This was due to the difference of Cu solubility in various systems at different reflow temperatures. The current study implied that the reflow process window should be tightly controlled.
- The consumption of Ni (V) UBM would change the failure mode from ductile (inside the bulk solder) to partial brittle (at interfaces) during ball shear tests

### ACKNOWLEDGEMENTS

The Flip Chip Division of K&S is acknowledged for providing the test dies. The authors are grateful to Professor K.N. Tu and Dr. K. Zeng for helpful discussions. Thanks are also due to DAGE-MPL Pte Ltd., Singapore for technical help in the ball shear tests.

### REFERENCES

1. *International Roadmap for Semiconductor Technology* (San Jose, CA: Semiconductor Industry Association, 1999), pp. 223–225.
2. K.N. Tu and K. Zeng, *Mater. Sci. Eng. R* 34, 1 (2001).
3. D.R. Frear, J.W. Jang, J.K. Lin, and C. Zhang, *JOM* 53 (6), 38 (2001).
4. S.-Y. Jang and K.-W. Paik, *Solder. Surf. Mount Technol.* 10, 29 (1998).
5. T.M. Korhonen, P. Su, S.J. Hong, M.A. Korhonen, and C.-Y. Li, *J. Electron. Mater.* 29, 1194 (2000).
6. T.M. Korhonen, P. Su, S.J. Hong, M.A. Korhonen, and C.-Y. Li, *Proc. 50th Electron. Comp. Technol. Conf.* 1106 (2000).
7. H.K. Kim, H.K. Liou, and K.N. Tu, *Appl. Phys. Lett.* 66, 2337 (1995).
8. R.S. Rai, S.K. Kang, and S. Purushothaman, *Proc. 45th Electron. Comp. Technol. Conf.* 1197 (1995).
9. J.W. Jang, P.G. Kim, K.N. Tu, D.R. Frear, and P. Thompson, *J. Appl. Phys.* 85, 8456 (1999).
10. C.Y. Liu, K.N. Tu, T.T. Sheng, C.H. Tung, D.R. Frear, and P. Elenius, *J. Appl. Phys.* 87, 750 (2000).
11. P.S. Teo, Y.W. Huang, C.H. Tung, M.R. Marks, and T.B. Lim, *Proc. 50th Electron. Comp. Technol. Conf.* 33 (2000).
12. K. Zeng, V. Vuorinen, and J.K. Kivilahti, *Proc. 51st Electron. Comp. Technol. Conf.* 693 (2001).
13. W.T. Chen, C.E. Ho, and C.R. Kao, *J. Mater. Res.* 17, 263 (2002).
14. J.W. Jang, A.P. De Silva, T.Y. Lee, J.K. Lin, and D.R. Frear, *Appl. Phys. Lett.* 79, 482 (2001).
15. H.K. Kim and K.N. Tu, *Phys. Rev. B* 53, 16027 (1996).
16. M. Schaefer, R.A. Fournelle, and J. Liang, *J. Electron. Mater.* 27, 1167 (1998).
17. K. Zeng and J.K. Kivilahti, *J. Electron. Mater.* 30, 35 (2001).
18. M. Li, F. Zhang, W.T. Chen, K. Zeng, K.N. Tu, H. Balkan, and P. Ellinus, *J. Mater. Res.* 17, 1612 (2002).